Efficient in vivo vascularization of tissue-engineering scaffolds. J Tissue Eng Regen Med. 2010 Sep 23.
30. Druecke D, Langer S, Lamme E, Pieper J, Ugarkovic M, Steinau HU, Homann HH. Neovascularization of poly(ether ester) block-copolymer scaffolds in vivo: long-term investigations using intravital fluorescent microscopy. J Biomed Mater Res A. 2004 Jan 1;68(1):10-8.
31. Ifkovits JL, Sundararaghavan HG, Burdick JA .Electrospinning fibrous polymer scaffolds for tissue engineering and cell culture. J Vis Exp. 2009 Oct 21;(32). pii: 1589.
32. Zhu X, Cui W, Li X, Jin Y. Electrospun fibrous mats with high porosity as potential scaffolds for skin tissue engineering. Biomacromolecules. 2008 Jul;9(7):1795-801.
33. Ju YM, Park K, Son JS, Kim JJ, Rhie JW, Han DK Beneficial effect of hydrophilized porous polymer scaffolds in tissue-engineered cartilage formation. J Biomed Mater Res B Appl Biomater. 2008 Apr;85(1):252-60.
34. Laschke MW, Strohe A, Scheuer C, Eglin D, Verrier S, Alini M, Pohlemann T, Menger MD. In vivo biocompatibility and vascularization of biodegradable porous polyurethane scaffolds for tissue engineering. Acta Biomater. 2009 Jul;5(6):1991-2001.
35. Lowery JL, Datta N, Rutledge GC. Effect of fiber diameter, pore size and seeding method on growth of human dermal fibroblasts in electrospun poly(epsilon-caprolactone) fibrous mats. Biomaterials. 2010 Jan;31(3):491-504.
36. Karageorgiou V, Kaplan D. Porosity of 3D biomaterial scaffolds and osteogenesis. Biomaterials. 2005 Sep;26(27):5474-91.
37. Mühl T, Binnebösel M, Klinge U, Goedderz T. New objective measurement to characterize the porosity of textile implants. J Biomed Mater Res B Appl Biomater. 2008 Jan;84(1):176-83.
38. Feng B, Jinkang Z, Zhen W, Jianxi L, Jiang C, Jian L, Guolin M, Xin D The effect of pore size on tissue ingrowth and neovascularization in porous bioceramics of controlled architecture in vivo. Biomed Mater. 2011 Feb;6(1):015007.
39. Cooper JA, Lu HH, Ko FK, Freeman JW, Laurencin CT Fiber-based tissue-engineered scaffold for ligament replacement: design considerations and in vitro evaluation. Biomaterials. 2005 May;26(13):1523-32.
40. Deng X, Guidoin R. Alternative blood conduits: assessment of whether the porosity of synthetic prostheses is the key to long-term biofunctionality. Med Biol Eng Comput. 2000 Mar;38(2):219-25.
41. Bragdon CR,Burke D,Lowenstein JD,O'Connor DO,Ramamurti B,Jasty M,Harris WH. Differences in stiffness of the interface between a cementless porous implant and cancellous bone in vivo in dogs due to varying amounts of implant motion. J Arthroplasty 1996;11(8): 945–951.
42. Zellin G, Linde A. Effects of different osteopromotive membrane porosities on experimental bone neogenesis in rats. Biomaterials 1996;17(7): 695–702.
43. Bertheville B. Porous single-phase NiTi processed under Ca reducing vapor for use as a bone graft substitute. Biomaterials 2006; 27(8): 1246–1250.
44. Stewart JD. Peripheral nerve fascicles: anatomy and clinical relevance. Muscle Nerve. 2003 Nov; 28(5):525-41.
45. Badia J, Pascual-Font A, Vivó M, Udina E, Navarro X. Topographical distribution of motor fascicles in the sciatic-tibial nerve of the rat. Muscle Nerve. 2010 Aug; 42(2):192-201.
46. Hallin RG. Microneurography in relation to intraneural topography: somatotopic organisation of median nerve fascicles in humans. J Neurol Neurosurg Psychiatry. 1990 Sep; 53(9):736-44.
47. Hallin RG, Wu G. Fitting pieces in the peripheral nerve puzzle. Exp Neurol. 2001 Dec; 172(2):482-92.

48. Okuyama N, Nakao Y, Takayama S, Toyama Y. Effect of number of fascicle on axonal regeneration in cable grafts. Microsurgery. 2004; 24(5):400-7.
49. Prodanov D, Feirabend HK. Morphometric analysis of the fiber populations of the rat sciatic nerve, its spinal roots, and its major branches. J Comp Neurol. 2007 Jul 1;503(1):85-100.
50. Wang W, Itoh S, Matsuda A, Aizawa T, Demura M, Ichinose S, Shinomiya K, Tanaka. J.Enhanced nerve regeneration through a bilayered chitosan tube: the effect of introduction of glycine spacer into the CYIGSR sequence. J Biomed Mater Res A. 2008 Jun 15;85(4):919-28.

Japanese Journal of Applied Physics 52 (2013) 07HF24 **REGULAR PAPER**
http://dx.doi.org/10.7567/JJAP.52.07HF24

Calibration Method in Elasticity Evaluation of Regenerating Cartilage Based on Ultrasonic Particle Velocity

Naotaka Nitta[1]*, Koji Hyodo[1], Masaki Misawa[1], Kazuhiko Hayashi[1], Yoshio Shirasaki[1], Kazuhiro Homma[1], and Tsuyoshi Shiina[2]

[1]*Human Technology Research Institute, National Institute of Advanced Industrial Science and Technology (AIST), Tsukuba, Ibaraki 305-8564, Japan*
[2]*Human Health Science, Graduate School of Medicine, Kyoto University, Kyoto 606-8507, Japan*
E-mail: n.nitta@aist.go.jp

Received November 23, 2012; accepted April 30, 2013; published online July 22, 2013

It is important in regenerative medicine to evaluate the maturity of regenerating tissue. In the maturity evaluation of regenerating cartilage, it is useful to measure the temporal change in elasticity because the maturity of regenerating tissue is closely related to its elasticity. In this study, a quantitative elasticity evaluation of extracted regenerating cartilage samples, which is based on the laser Doppler measurement of ultrasonic particle velocity and calibration, was experimentally investigated using agar-based phantoms with different Young's moduli and regenerating cartilage samples extracted from beagles in animal experiments. The experimental results verified the feasibility of the proposed method for the elasticity evaluation of regenerating cartilage samples. © 2013 The Japan Society of Applied Physics

1. Introduction

The quantitative evaluation of cartilage has become important with the aging of the population. For example, osteoarthritis (OA) is one of the most common disorders found in elderly people. In degenerative cartilage, the tension of the superficial layer of the collagen fiber decreases gradually.[1–4] The status of cartilage is evaluated with various methodologies. For in vitro evaluations of cartilage using ultrasound, acoustic microscopy,[5–8] sound speed measurement,[9–12] attenuation measurement,[13] reflected wave or backscatter analysis,[14–19] and an elastographic compressive approach based on echo shift measurement due to cartilage compression,[20,21] have been studied. For in vivo evaluations of cartilage, reflected wave analysis, evaluation of the roughness of the cartilage surface, thickness measurement, and power Doppler evaluation using an ultrasound diagnosis device have been studied.[22–26] Moreover, as a less invasive approach, reflected wave analysis using intravascular ultrasound has also been studied.[27] A more direct approach for mechanical property assessment is a mechanical compression-based method. One of the most important properties of cartilage is its mechanical property including elasticity or viscoelasticity. Therefore, some methods[28–30] might also be promising for evaluating the mechanical properties of cartilage. However, since no speckle pattern typically appears in an ultrasound image of cartilage, it would be difficult for elasticity imaging methods based on speckle tracking to evaluate the elasticity of cartilage.

On the other hand, as a solution to recover degenerated or deficient cartilage, regenerative medicine has been addressed. In typical regenerative medicine for cartilage recovery, a cell-seeded scaffold is cultured over a period of time and then the cultured scaffold is transplanted into the body. Here, evaluations of the cultured scaffold before and after transplantation are essential for ensuring its adequate maturity before and after transportation. In the maturity evaluation of regenerating cartilage, it is useful to measure the temporal change in elasticity because the maturity of regenerating tissue is closely related to its elasticity. For the maturity evaluation, sound speed and attenuation measurements using acoustic microscopy has been reported.[31] On the other hand, since the cultured scaffold before transplantation is the sole material, nondestructive and noncontact measurements are required for elasticity evaluation.

Therefore, with the evaluation of a cultured scaffold sample before transplantation in mind, we previously proposed an elasticity evaluation method for extracted regenerating cartilage samples, which is based on ultrasound particle velocity measurement using a laser Doppler vibrometer (LDV).[32] In our previous study, a relative elasticity evaluation was performed using the inverse of strain (IS) as an index. However, for quantitative evaluations, calibration is required. In this study, a quantitative elasticity evaluation method for extracted regenerating cartilage samples, which is based on the laser Doppler measurement of ultrasonic particle velocity and calibration, was experimentally investigated using agar-based phantoms with different elastic moduli and regenerating cartilage samples extracted from beagles in animal experiments.

2. Calibration Method

In this study, with the aim of simplifying the problem of elasticity evaluation for cartilage tissue, the cartilage tissue is assumed to be a nearly incompressible, isotropic and linear elastic body. In other words, it is assumed that the effect of shear modulus is sufficiently small and negligible, although it is not zero.

Figure 1 shows the principle of the proposed method. Here, a series of ultrasound pulses are irradiated from the bottom of the sample and the particle velocity on the sample surface is measured. Here, only the longitudinal wave propagation is considered, and it is assumed that the whole cartilage tissue sample is homogeneous. Since the particle velocity is continuous at the boundary between media with different acoustic impedances, the particle velocity measured at the surface boundary of the sample is equivalent to that inside the sample. From the above assumptions, when only the plane progressive wave of longitudinal waves propagates in the homogeneous cartilage sample, the particle velocity v_i is expressed as

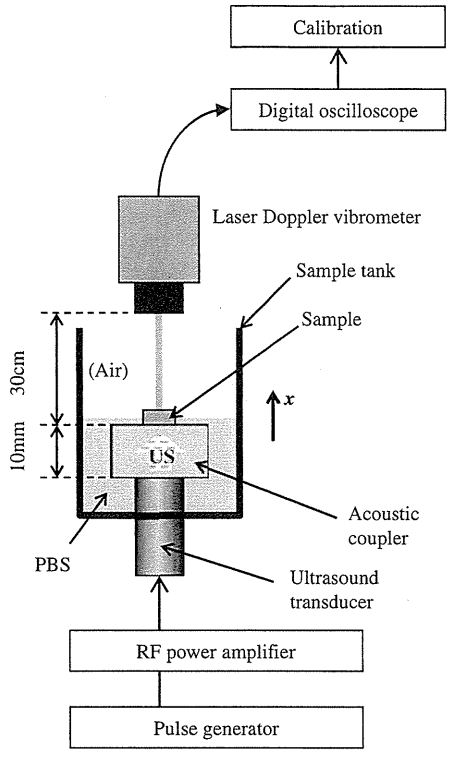

Fig. 1. Setup for laser Doppler measurement of ultrasound particle velocity.

$$v_i = \sqrt{2}v_i' e^{j\omega_0 t}, \tag{1}$$

where v_i', ω_0, and t indicate the effective value of particle velocity, angular frequency, and time, respectively. The index i of v_i' means the incident wave, that is, a progressive wave in the sample. v_i' is a function of position x along the direction of longitudinal wave propagation, as shown in Fig. 1. In this paper, the effective value is expressed as a complex number.

Next, the particle displacement u_i is derived by integrating the particle velocity v_i with respect to time as

$$u_i = \sqrt{2}u_i' e^{j\omega_0 t}, \tag{2}$$

where u_i' $(= -jv_i'/\omega_0)$ is the effective value of particle displacement and a function of x. In order to attain elasticity information, the strain ε_i' is derived by differentiating u_i' with respect to x. However, since the laser Doppler measurement in Fig. 1 is conducted at only one point on the surface boundary of the sample, the above-mentioned strain $|\varepsilon_i'|$ is approximated by using the simultaneously measured sample thickness l as

$$|\varepsilon_i'| = \frac{|u_i'|}{l}. \tag{3}$$

This processing corresponds to the calculation of average strain inside the sample when it is assumed that the displacement at the bottom boundary of the sample is zero. In the previous study,[32] the inverse of the above average strain was referred to as the IS and the relative elasticity evaluation was performed.

On the other hand, the bulk modulus K is derived by calculating the ratio of the stress σ_i' to the strain ε_i' as

$$K = \frac{|\sigma_i'|}{|\varepsilon_i'|}, \tag{4}$$

where σ_i' is deemed as the stress on the surface of the cartilage sample. Therefore, the stress is affected by the acoustic impedances of the sample and surrounding media. Here, the transmission coefficient T_p of the stress σ_{1i}' induced by the incident wave in the coupler is expressed as

$$|T_p| = \frac{|\sigma_i'|}{|\sigma_{1i}'|}, \tag{5}$$

where σ_{1i}' is a constant when the amplitude of the input voltage applied to the ultrasound transducer is constant. By substituting Eq. (5) into Eq. (4) and rewriting the bulk modulus K as the Young's modulus E by using the relation $K = E/[3(1-2\nu)]$ (ν: Poisson's ratio), the following equation is derived.

$$E = C \cdot \mathrm{IS}. \tag{6}$$

Here, the coefficient C is defined as

$$C = 3(1-2\nu)|T_p||\sigma_{1i}'|. \tag{7}$$

Thus, the coefficient C is composed of Poisson's ratio, the transmission coefficient, and the stress induced by the incident wave in the coupler. However, since Poisson's ratio and the transmission coefficient are dimensionless, the coefficient C has the same dimension as the stress on the surface of the sample. To convert the IS into E, the uniqueness of C is investigated in the following discussion. Here, the transmission coefficient is derived as[32]

$$|T_p| = \frac{2}{\sqrt{\left(1+\frac{Z_1}{Z_3}\right)^2 \cos^2(kl) + \left(\frac{Z_2}{Z_3}+\frac{Z_1}{Z_2}\right)^2 \sin^2(kl)}}, \tag{8}$$

where Z_1, Z_2, and Z_3 are the acoustic impedances in the coupler, regenerating cartilage sample, and air, respectively. k and l are the wavelength constant and the thickness of the sample, respectively. Variations in $|T_p|$ to the Young's modulus E of regenerating cartilage samples were simulated, as shown in Fig. 2. Here, the horizontal and vertical axes indicate E and $|T_p|$, respectively. Assuming that the frequency of 1 MHz was used, $|T_p|$ values for sample thickness l of 1 or 5 mm were exhaustively calculated by substituting the acoustic impedances of the coupler and air ($Z_1 = 1.01 \times 10^3\,\mathrm{kg/m^3} \times 1519\,\mathrm{m/s} = 1.53 \times 10^6\,\mathrm{kg{\cdot}m^{-2}{\cdot}s^{-1}}$, $Z_3 = 1.2\,\mathrm{kg/m^3} \times 343\,\mathrm{m/s} = 412\,\mathrm{kg{\cdot}m^{-2}{\cdot}s^{-1}}$) and various acoustic impedances $Z_2 = \rho_2 c_2$ (ρ_2: density, and c_2: sound speed) of the sample within the realistic range for native and regenerating cartilages into Eq. (8). Specifically, densities ρ_2 of 1.00×10^3 to $1.02 \times 10^3\,\mathrm{kg/m^3}$ and sound speeds c_2 of 1500 to 2000 m/s were used. In addition, Young's moduli of 10^{-5} to 5 MPa were also used in relation to the given density and speed sound. Then, Poisson's ratio is calculated uniquely by using the relationship $\nu = 0.5 - E/(6\rho_2 c_2)$. In Fig. 2, although there is no correlation between $|T_p|$ and E ($R^2 = 1 \times 10^{-18}$ for $l = 1$ mm, and $R^2 = 6 \times 10^{-17}$ for $l = 5$ mm), each $|T_p|$ has fluctuations around a constant mean value caused by variations in density and sound speed. From the mean value and standard deviation (SD) of $|T_p|$ shown in Fig. 2, the

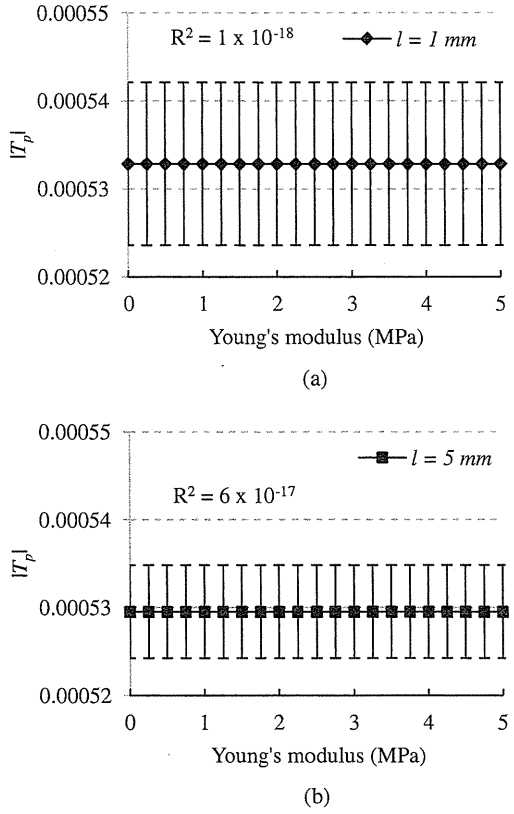

Fig. 2. Relationship between the Young's modulus E (horizontal line) and the transmission coefficient $|T_p|$ (vertical line) in samples with thickness l. (a) and (b) show the mean value and SD of $|T_p|$ for $l = 1$ and 5 mm, respectively. The CVs of $|T_p|$ in (a) and (b) are 1.7 and 0.9%, respectively.

coefficients of variance (CVs) (= 100 × SD/mean) were 1.7% for $l = 1$ mm and 0.9% for $l = 5$ mm. The CV corresponds to the error rate in the calculation of Young's modulus when $|T_p|$ is regarded as a constant. Next, the mean and SD of the collaterally obtained Poisson's ratio in the above calculation process were 0.499 and 9.04×10^{-5}, respectively. Consequently, when the above fluctuations in both $|T_p|$ and Poisson's ratio are considered, the CV of C reaches 64.8%. This means that large errors occur in the calculation of Young's modulus using a constant C, when both $|T_p|$ and Poisson's ratio are unknown.

In order to avoid this problem, it is effective that the coefficient C is determined by using test materials for calibration with the same or a similar Poisson's ratio to that of regenerating cartilage. Since the CV of C decreases to that of $|T_p|$ as a result of such determination, the use of C as the calibration coefficient becomes realistic and valid for the quantitative elasticity evaluation.

Another merit of using test materials is that a sampling test using the regenerating cartilage itself can be avoided. Since the cultured regenerating cartilage is a valuable sole material and cannot be used for the sampling test, the coefficient C cannot be determined by using the regenerating cartilage itself. In addition, the stress information required for Young's modulus estimation can also be obtained by the determination of C using the test materials. In this case, the input voltage to the ultrasound transducer and the stress $|\sigma'_{1i}|$ must be maintained constant.

In this study, the calibration coefficient is determined experimentally by comparing the Young's moduli measured by mechanical tests and the ISs measured by our previously proposed method using test materials.

3. Experimental Setup

Figure 1 also shows the measurement system used in this study. A cylindrical sample tank contains phosphate buffered saline (PBS) whose temperature was kept at 20.0 °C. In the sample tank, a circular urethane-based acoustic coupler (Takiron STD112) with a thickness of 10 mm and a diameter of 20 mm was placed on the surface of an ultrasound transducer with a planar aperture, a center frequency of 1 MHz, and a circular element with a diameter of 6 mm (GE Sensing and Inspection Tech. 221-340), and an extracted regenerating cartilage sample was placed on the acoustic coupler. A laser Doppler vibrometer (LDV; Graphtec AT0023 and AT3700) with a spot diameter of 20 μm and a frequency range up to 10 MHz was set 30 cm apart from the cartilage sample surface. The laser spot of the LDV was also positioned on the central axis of the acoustic field by irradiating a visible red laser beam (wavelength: 632.8 nm) at the aperture center of the ultrasound transducer before placing the coupler on the transducer. On the basis of such settings, the measuring point and central axis of acoustic field on the sample surface can be easily identified when the sample is placed on the coupler.

After completing the above setup, pulsed-wave ultrasound with a wave number of 5 was irradiated to the bottom of the cartilage sample via the acoustic coupler. The voltage applied to the ultrasound transducer was 450 V_{pp} and was maintained constant. This acoustic output generated a particle displacement of 0.46 μm on the surface of the acoustic coupler without the sample placed on it, as determined by the root mean square (RMS) calculation for the particle displacement waveform. Then, the LDV measured the ultrasound particle velocity on the surface of the cartilage sample, and the particle velocity waveforms were recorded using a digital oscilloscope (LeCroy WS454VL) at a sampling frequency of 500 MHz. After recording the data, the particle velocity waveform was converted to the particle displacement waveform by temporal integration. Then, $|u'_i|$ in Eq. (3) was obtained by calculating the RMS of the particle displacement waveform. The calculation of RMS was also effective for obtaining a high signal-to-noise ratio. At the same time, the thickness of the sample, l in Eq. (3), was also measured using a laser thickness indicator (KEYENCE LK-G35). Subsequently, the IS, that is, $1/|\varepsilon'_i|$, was calculated using Eq. (3).

On the other hand, in order to determine the calibration coefficient, the reference Young's modulus was also measured by a static mechanical compression test. This test was conducted using an Instron-type universal testing machine (A&D UTM-10T). The sample was quasi-statically compressed by a plate-type indenter with a diameter of 10 mm at a constant crosshead speed of 2 mm/min, and simultaneously, the compression forces were measured by a load cell (rating capacity of 1 kg, and resolution of 0.02% of rating capacity). Stress and strain were calculated from the measured forces and the dimensions of the sample, and then the Young's modulus of the sample was calculated using the

ratio of stress to strain. In the same test materials, both the static mechanical compression test and the IS measurement were conducted and the calibration coefficient was determined by comparing these values. For the regenerating cartilage sample, first, the IS was measured and then Young's modulus was calculated using the predetermined calibration coefficient.

4. Results

4.1 Determination of calibration coefficient

To determine the calibration coefficient in this study, three homogeneous phantoms with different elasticities (0.05, 0.1, and 0.2 MPa as Young's moduli) and a constant size (side length of 10 mm, and thickness of 5 mm) were made by changing the weight concentration of agar powder and used as the test materials. For each phantom, the IS was measured by our previously proposed method, and the reference Young's modulus was measured by the static compression test described in Sect. 3. On the basis of manufacturing these agar-based phantoms, the densities of the agar-based phantoms with Young's moduli of 0.05, 0.1, and 0.2 MPa were 1.01×10^3, 1.02×10^3, and 1.02×10^3 kg/m^3, respectively. Likewise, the sound speeds of the agar-based phantoms with Young's moduli of 0.05, 0.1, and 0.2 MPa were 1520, 1532, and 1556 m/s, respectively.[32] The calculation of Poisson's ratio described in Sect. 2 revealed that the Poisson's ratio in the agar-based phantoms was 0.499. By comparison, the density and sound speed in the specimen of native auricular cartilage tissue of a beagle were measured to be 1.02×10^3 kg/m^3 and 1599 m/s, respectively.[32] In addition, the Young's modulus in the specimen was 0.5 MPa. As a result, the Poisson's ratio of this native cartilage tissue was 0.499. Namely, there was no significant difference between the Poisson's ratios of the agar-based phantoms and the native cartilage tissue. It is predicted that the acoustic properties and Young's modulus of the regenerating cartilage tissue will gradually become close to those of the native cartilage tissue. Therefore, it is also predicted that there will be no significant difference between the Poisson's ratios of the agar-based phantoms and the regenerating cartilage tissue. Consequently, the use of these agar-based phantoms is appropriate and valid for the determination of the calibration coefficient.

Figure 3 shows a comparison of the reference Young's moduli with the ISs ($n = 3$). A linear relationship between the reference Young's modulus and the IS was observed. The slope of this straight line corresponds to the calibration coefficient. Therefore, the calibration coefficient was determined by fitting a linear regression line to the measured points in Fig. 3.

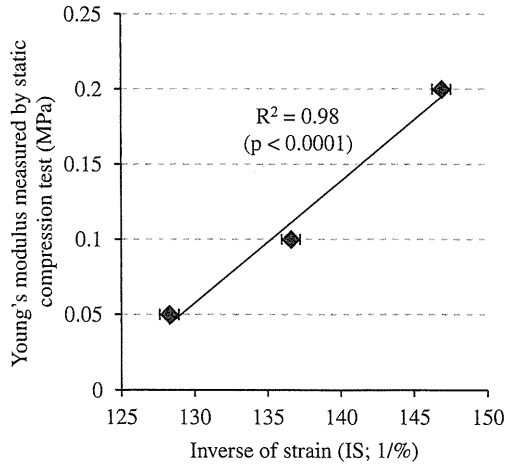

Fig. 3. Determination of calibration coefficient using agar-based phantoms with different Young's moduli.

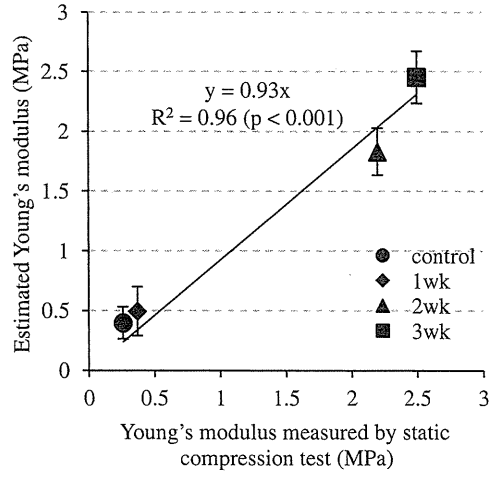

Fig. 4. Calibration results for regenerating cartilage sample elasticities.

4.2 Regenerating cartilage sample measurement

In vitro measurements using regenerating cartilage samples ($n = 3$), which were extracted from beagles in approved animal experiments, were conducted using the above-mentioned system. Autologous auricular cartilage cells of a beagle were transfused into a poly(L-lactic acid) (PLLA) scaffold and cultured for a certain period of time (1, 2, or 3 weeks). The scaffold with the cultured cells was transplanted subcutaneously in the same beagle and extracted after 2 months. The extracted cartilage sample (side length of 5 mm, and thickness of 1 mm) was placed on the acoustic coupler, and the IS was measured by our method. Here, although the thickness of the cartilage sample was 1 mm, the thickness of the above agar-based phantom was 5 mm because of ease in making homogeneous phantoms. However, there was no significant difference between $|T_p|$ for $l = 1$ mm and that for $l = 5$ mm, as shown in Fig. 2. Therefore, the Young's moduli of the cartilage samples were determined using the measured ISs in the samples and the predetermined calibration coefficient in the agar-based phantoms.

Figure 4 shows the calibration results for regenerating cartilage sample elasticities for various culture periods (1, 2, and 3 weeks). As a reference, control data were also acquired using only the scaffold without any cell seed. A relatively high correlation and good agreement between the calibrated Young's moduli and the Young's moduli measured by the mechanical compression test were observed.

5. Conclusions

A calibration method for quantitative elasticity evaluation of

a regenerating cartilage sample was proposed and investigated using agar-based phantoms and regenerating cartilage samples. Experimental results obtained using regenerating cartilage samples revealed the feasibility of the proposed calibration method. In this method, the stability of test materials and the accuracies of the IS measurement and mechanical test are important. Therefore, in future works, the accuracy of the calibration method must be improved through measurements using a number of test materials for calibration.

Acknowledgments

This work was supported by the Research and Development of Three-dimensional Complex Organ Structures, NEDO, Japan, and the Grant-in-Aid for Scientific Research (A) (22240063) from the Japan Society for the Promotion of Science (JSPS). We appreciate Dr. Hoshi of the University of Tokyo who supplied us with the valuable regenerating cartilage samples in animal experiments.

1) C. G. Armstrong and V. C. Mow: J. Bone Joint Surg. Am. **64** (1982) 88.
2) J. S. Wayne, K. A. Kraft, K. J. Shields, C. Yin, J. R. Owen, and D. G. Disler: Radiology **228** (2003) 493.
3) L. P. Li, W. Herzog, R. K. Korhonen, and J. S. Jurvelin: Med. Eng. Phys. **27** (2005) 51.
4) L. P. Li, R. K. Korhonen, J. Iivarinen, J. S. Jurvelin, and W. Herzog: Med. Eng. Phys. **30** (2008) 182.
5) Q. Wang and Y.-P. Zheng: Ultrason. Med. Biol. **35** (2009) 1535.
6) E. H. Chiang, T. J. Laing, C. R. Meyer, J. L. Boes, J. M. Rubin, and R. S. Adler: Ultrason. Med. Biol. **23** (1997) 205.
7) M. H. Lu, Y. P. Zheng, and Q. H. Huang: Ultrason. Med. Biol. **31** (2005) 817.
8) S.-Z. Wang, Y.-P. Huang, S. Saarakkala, and Y.-P. Zheng: Ultrason. Med. Biol. **36** (2010) 512.
9) H. J. Nieminen, P. Julkunen, J. Töyräs, and J. S. Jurvelin: Ultrason. Med. Biol. **33** (2007) 1755.
10) J.-K. F. Suh, I. Youn, and F. H. Fu: J. Biomech. **34** (2001) 1347.
11) J. Töyräs, M. S. Laasanen, S. Saarakkala, M. J. Lammi, J. Rieppo, J. Kurkijärvi, R. Lappalainen, and J. S. Jurvelin: Ultrason. Med. Biol. **29** (2003) 447.
12) S. G. Patil, Y. P. Zheng, and X. Chen: Ultrason. Med. Biol. **36** (2010) 1345.
13) H. J. Nieminen, S. Saarakkala, M. S. Laasanen, J. Hirvonen, J. S. Jurvelin, and J. Töyräs: Ultrason. Med. Biol. **30** (2004) 493.
14) S. Saarakkala, M. S. Laasanen, J. S. Jurvelin, K. Törrönen, M. J. Lammi, R. Lappalainen, and J. Töyräs: Osteoarthritis Cartilage **11** (2003) 697.
15) P. Kiviranta, E. Lammentausta, J. Töyräs, I. Kiviranta, and J. S. Jurvelin: Osteoarthritis Cartilage **16** (2008) 796.
16) A. S. Aula, J. Töyräs, V. Tiitu, and J. S. Jurvelin: Osteoarthritis Cartilage **18** (2010) 1570.
17) B. Pellaumail, A. Watrin, D. Loeuille, P. Netter, G. Berger, P. Laugier, and A. Saïed: Osteoarthritis Cartilage **10** (2002) 535.
18) S. Saarakkala, S.-Z. Wang, Y.-P. Huang, J. S. Jurvelin, and Y.-P. Zheng: Ultrason. Med. Biol. **37** (2011) 112.
19) K. Hattori, K. Mori, T. Habata, Y. Takakura, and K. Ikeuchi: Clin. Biomech. **18** (2003) 553.
20) M. Fortin, M. D. Buschmann, M. J. Bertrand, F. S. Foster, and J. Ophir: J. Biomech. **36** (2003) 443.
21) Y. P. Zheng, H. J. Niu, F. T. Arthur Mak, and Y. P. Huang: J. Biomech. **38** (2005) 1830.
22) M. S. Laasanen, J. Töyräs, A. Vasara, S. Saarakkala, M. M. Hyttinen, I. Kiviranta, and J. S. Jurvelin: Osteoarthritis Cartilage **14** (2006) 258.
23) S. Saarakkala, J. Töyräs, J. Hirvonen, M. S. Laasanen, R. Lappalainen, and J. S. Jurvelin: Ultrason. Med. Biol. **30** (2004) 783.
24) C.-Y. Tsai, C.-L. Lee, C.-Y. Chai, C.-H. Chen, J.-Y. Su, H.-T. Huang, and M.-H. Huang: Osteoarthritis Cartilage **15** (2007) 245.
25) J. Töyräs, T. Lyyra-Laitinen, M. Niinimäki, R. Lindgren, M. T. Nieminen, I. Kiviranta, and J. S. Jurvelin: J. Biomech. **34** (2001) 251.
26) L. Mancarella, M. Magnani, O. Addimanda, E. Pignotti, S. Galletti, and R. Meliconi: Osteoarthritis Cartilage **18** (2010) 1263.
27) T. Virén, S. Saarakkala, E. Kaleva, H. J. Nieminen, J. S. Jurvelin, and J. Töyräs: Ultrason. Med. Biol. **35** (2009) 1546.
28) M. Yamakawa and T. Shiina: Jpn. J. Appl. Phys. **51** (2012) 07GF12.
29) T. Miwa, Y. Yoshihara, K. Kanzawa, R. Kumar Parajuli, and Y. Yamakoshi: Jpn. J. Appl. Phys. **51** (2012) 07GF13.
30) T. Sato, Y. Watanabe, and H. Sekimoto: Jpn. J. Appl. Phys. **51** (2012) 07GF16.
31) Y. Tanaka, Y. Saijo, Y. Fujihara, H. Yamaoka, S. Nishizawa, S. Nagata, T. Ogasawara, Y. Asawa, T. Takato, and K. Hoshi: J. Biosci. Bioeng. **113** (2012) 252.
32) N. Nitta, M. Misawa, K. Homma, and T. Shiina: Jpn. J. Appl. Phys. **51** (2012) 07GF15.

Radiol Phys Technol (2013) 6:480–485
DOI 10.1007/s12194-013-0223-4

Non-invasive speed of sound measurement in cartilage by use of combined magnetic resonance imaging and ultrasound: an initial study

Takako Aoki · Naotaka Nitta · Akira Furukawa

Received: 26 December 2012 / Revised: 20 May 2013 / Accepted: 21 May 2013 / Published online: 1 June 2013

Abstract The speed of sound (SOS) is available as an index of elasticity. Using a combination of magnetic resonance imaging (MRI) and ultrasound, one can measure the SOS. In this study, we verified the accuracy of SOS measurements by using a combination of MRI and ultrasound. The accuracy of the thickness measurements was confirmed by comparison of the results obtained with use of MRI with those of a non-contact laser, and the accuracy of the calculated SOS values was confirmed by comparison of the results of the combined method and ultrasound measurements with the transmission method ex vivo. There was no significant difference between thickness measurements by MRI and those with the non-contact laser, and there was a significant linear correlation between SOS measurement results by use of the combined method and those by use of the transmission method. We also showed that the SOS values obtained agreed with those of previously published studies.

T. Aoki (✉)
Department of Radiological Science, Graduate School of Human Health Science, Tokyo Metropolitan University,
7-2-10 Higashiogu, Arakawa-ku, Tokyo 116-855, Japan
e-mail: t.aoki360@gmail.com

N. Nitta
Human Technology Research Institute, National Institute of Advanced Industrial Science and Technology (AIST), Tsukuba, Ibaraki, Japan

A. Furukawa
School of Radiological Science, Faculty of Health Sciences, Tokyo Metropolitan University, Tokyo, Japan

Keywords Articular cartilage · Cartilage thickness · Elasticity · Osteoarthritis · Magnetic resonance imaging · Speed of sound

1 Introduction

The onset of osteoarthritis (OA) due to aging involves biological change, mechanical property change, and structural change in the cartilage. The speed of sound (SOS) in tissue varies according to the pathologic condition in a disease [1–3], and is available as an index of tissue elasticity, which is helpful in the differential diagnosis. Ghoshal et al. [4] reported that the SOS in the liver decreased as the fat content increased. Kiviranta et al. [5] investigated the SOS in cartilage and described the relationship between tissue stiffness and the SOS in the tissue, as demonstrated by measurements use of ultrasound-indentation method in a study that used various high-frequency ultrasound measurements for obtaining elasticity indices ex vivo. An accurate method for measuring the SOS in cartilage would be valuable for diagnosing OA, especially if it could be applied to measurements in vivo.

Conventional ultrasound elastography imaging with phase-sensitive speckle-tracking algorithms has been used as a non-invasive method for evaluating elasticity in several types of tissue [6, 7], but the lack of an internal signal in tissue such as cartilage makes imaging difficult. However, the assessment of ultrasound imaging has been improved by the advent of the pulse-echo method [8]. Use of the pulse-echo method with wide dynamic range enables visualization of tissue boundaries such as that between the bone and cartilage with a high signal intensity image [8].

In this study, we evaluated our proposed method, which combines magnetic resonance imaging (MRI) and

pulse-echo ultrasound measurements for SOS measurements in cartilage.

2 Materials and methods

2.1 Specimen preparation

Three-percent (w/v) agar phantoms ($n = 10$), approximately 5 mm in thickness, were made from agar powder in a laboratory dish (Wako Pure Chemical Industries, Osaka, Japan) dissolved in heated deionized water, with glycerin added in concentrations ranging from 10 to 60 % (w/v) (Wako Pure Chemical Industries). The SOS in agar phantoms varies according to the concentration of glycerin [9], and the phantoms made for this study incorporated different concentrations of glycerin, in steps of 5 %.

Fresh porcine knee joints ($n = 6$) were obtained from a local abattoir (ZEN-NOH Central Research Institute for Feed and Livestock, Ibaraki, Japan). From each specimen, disks 12 mm in diameter (total, $n = 24$) were harvested from four sites on the medial and lateral femoral condyles. The subchondral bone was removed from each specimen with a punch and a razor [10]. MRI and pulse-echo ultrasound measurements were performed with the specimens encased in agar. Table 1 shows a description of the subjects and measurements.

2.2 MRI imaging

MRI was performed with a 3.0T whole-body clinical scanner (InteraAchieva; Philips Medical Systems, Best, Netherlands) with a sensitivity encoding (SENSE) coil for wrists with use of a parallel imaging technique. Morphological isotropic voxel images were acquired using a three-dimensional (3D) fast-field echo (FFE) sequence with the following parameters: repetition time/echo time (TE1/TE2), 19/7.0/13.3 ms; field of view, 80 × 80 mm; flip angle, 35°; scanned matrix, 512 × 512 (acquired matrix 256 × 256); slice number, 230; voxel size, 0.3 mm^3; and number of excitations, 1. Reduction factors for parallel imaging were 1 (phase direction) and 2 (slice direction). Fat suppression was achieved with the use of water excitation (total scan duration: 309 s). The FFE sequence has several different types of contrasts, and we used 'm-FFE', which meant multi-slice, multi-echo sequence. The image of TE2 was used for measurement of the cartilage thickness.

2.3 Theory supporting SOS measurements in cartilage by use of the combined method

The distance between two points when ultrasound imaging is used is calculated from the time of flight (TOF) of an ultrasound pulse between two points, by use of a fixed value for the SOS, as shown in Eq. (1). In Japanese ultrasound devices, this fixed SOS value is set as 1530 m/s, in accordance with Japanese industrial standards.

$$\text{Distance} = \text{SOS}_{(\text{fixed})} \times \text{TOF}, \quad (1)$$

where TOF represents the flight time of the ultrasound pulse between the two points. Then, after the cartilage thickness is accurately measured by MRI, an actual SOS value for the cartilage specimen can be calculated as follows.

$$\text{SOS}_{(\text{cartilage})} = \text{SOS}_{(\text{fixed})} \times \text{Thickness}_{(\text{MRI})}/\text{Thickness}_{(\text{ultrasound})}, \quad (2)$$

where '$\text{SOS}_{(\text{cartilage})}$' is the actual SOS in the cartilage, '$\text{SOS}_{(\text{fixed})}$' is the set 1530 m/s value used in the device, and '$\text{Thickness}_{(\text{MRI})}$' and '$\text{Thickness}_{(\text{ultrasound})}$' are the cartilage thicknesses measured by MRI and by ultrasound, respectively.

2.4 Theory supporting SOS measurements in cartilage by transmission method

The SOS was calculated for agar phantoms with the following formulas, where l is the distance between

Table 1 Description of the subjects and measurements

Subject	Number	Preparation	Measurement	
			Target	Method
3 %-agar + glycerin added phantoms	10	Quantity of glycerin addition (g/100 ml) 0, 10, 15, 20, 25, 30, 35, 40, 45, 50, 60 Approx. 5 mm thickness, in a laboratory dish	Exact subject's thickness Subject's thickness and speed of sound	Non-contact laser Ultrasound (transmission) Ultrasound (pulse-echo) and MRI
Porcine knee cartilage specimen	24 6 knees 4 sites	Disks 12 mm in diameter Medial and lateral femoral condyles		Ultrasound (pulse-echo) and MRI

transducer 1 and transducer 2 (30 mm), l_1 is the distance between the transducer and the agar phantom, l_2 is the thickness of the agar phantom, c_0 and c are the SOS of saline and the agar phantom, and t and t_0 are one-way TOF when the agar phantom is placed between the transducers and when it is not placed, respectively (Fig. 1).

$$l = l_1 + l_2 \tag{6}$$

$$t = l_2/c + l_1/c_0 \tag{7}$$

$$t_0 = l/c_0 \tag{8}$$

Hence, the SOS in an agar phantom can be calculated from the following formula:

$$c = 1/((t - t_0)/l_2 + 1/c_0). \tag{9}$$

2.5 Thickness measurements of specimens

The accuracy of cartilage thickness measurements was evaluated with agar phantoms and porcine knee cartilage specimens by use of the following modalities: pulse-echo ultrasound measurements, with a center frequency of 10 MHz and a fixed SOS (EUB-7500; Hitachi Medical Corporation, Tokyo, Japan); MRI as described above; a non-contact laser (spot diameter, 70 μm; LK-G35, LKGD500, Keyence, Japan). The laser we used was a type to measure distance from surface reflection which can measure the agar, but the cartilage specimen had difficulty in laser measurement for its milky-white color. In the pulse-echo ultrasound measurements, the cartilaginous thickness was obtained from the distance between the peaks of the profile curve (Fig. 2a). In MRI measurements of thickness, agar phantom thicknesses were obtained by use of the full width at half maximum (FWHM, Fig. 2b) with a square region of interest (ROI) parallel to the phantom's surface. The thicknesses of the cartilage specimens were obtained from the distance between the peaks of the profile curve, with use of manual outline extraction. All thickness measurements were reprocessed with Image J software (version 1.45, National Institutes of Health, Bethesda, Maryland, USA). Because the repetitive accuracy of laser measurements is of the order of 0.05 μm, the thickness measurements obtained by the laser device were considered gold standard values. Each thickness measurement was performed five times, and the mean values of these measurements were used in this study.

2.6 SOS measurements in specimens

The SOS in cartilage specimens was measured with the combination of pulse-echo ultrasound and MRI, as described above, and also with transmission ultrasound. Because the SOS calculated from the TOF which was obtained by transmission ultrasound measurements was considered the gold standard value, the SOS values for the agar phantoms obtained by transmission ultrasound measurements alone were compared with those obtained via the combined method. And the SOS values of the porcine cartilage specimens calculated from the combined method were compared with values of previous studies.

The transmission ultrasound method was implemented with planar non-focusing transducers with a center frequency of 5 MHz and an aperture diameter of 0.25 in. (GE Inspection Technologies, Wichita, KS, USA), by use of a non-contact method [11] at room temperature (18.4 °C). The multiple pulses of TOF which were obtained from an oscilloscope were averaged to raise the measurement

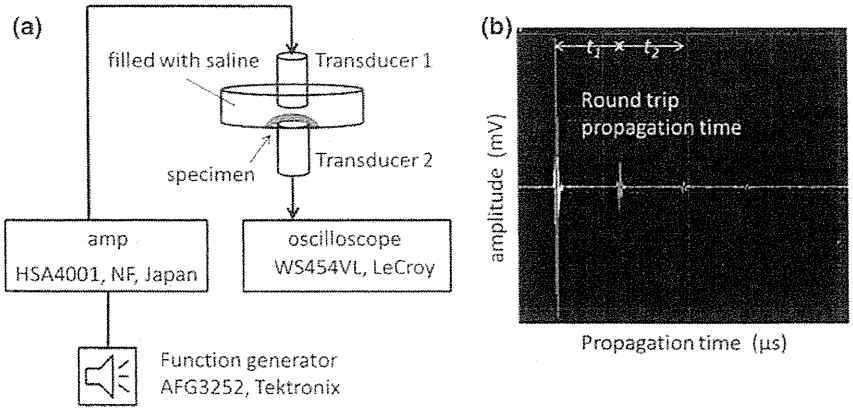

Fig. 1 Cartilaginous SOS measurements by use of transmission ultrasound. A cartilage specimen is placed in a laboratory dish filled with saline. Ultrasonic waves from transducer 1 penetrate the specimen and are received by transducer 2. **a** The one-way TOF is measured with an oscilloscope; **b** measuring and averaging the times between multi-echoes yields high-precision measurement of propagation time (t). $t = (t_1 + t_2)/2$. t_1: 1st–2nd wave; t_2: 2nd–3rd wave. The unit of propagation in the figure, "μs", means microsecond, and the unit of amplitude "mV", means millivolt